

2. METHODS OF INVESTIGATING THE CIRCUMSTANCES OF APPROVALS IN THE THREE REGIONS

For the approval situation in Japan, we investigated review reports obtained from the website of the Pharmaceuticals and Medical Devices Agency (http://www.info.pmda.go.jp/shinyaku/shinyaku_index.html). Regarding the US, we extracted brand names of NMEs from the FDA's CDER Drug and Biologic Approval Reports (<http://www.fda.gov/cder/rdmt/>). We also examined approval history obtained from Drugs@FDA (<http://www.accessdata.fda.gov/scripts/cder/drugsatfda/index.cfm>). For the EU, we extracted brand names of NMEs through the Centralized Approval Process from the Community Register of medicinal products (<http://ec.europa.eu/enterprise/pharmaceuticals/register/index.htm>) provided by the European Commission, and investigated product overview on target drugs from the EMEA's EPARs for authorized medicinal products for human use (<http://www.emea.europa.eu/htms/human/epar/a.htm>).

Table 1. NMEs approved in Japan, US and EU in 2006

Japan	US	EU
Aripiprazole	Sunitinib	Daptomycin
Silodosin	Ranolazine	Human normal Ig
Letrozole	Lubiprostone	Galsulfase
Clopidogrel	Anidulafungin	Fentanyl
Follitropin Alfa	Decitabine	Pegaptanib
Cetorelix	Varenicline	Rotigotine
Tolterodine	Rasagiline	Alglucosidase alfa
Sertraline	Darunavir	Tigecycline
Solifenacin	Dasatinib	Timolol
Gabapentin	Avobenzone	Parathyroid hormone
Mozavaptane	Ecamsule	Clofarabine
Temozolomide	Octocrylene	Rimonabant
Interferon Beta-1a	Posaconazole	Entecavir
Entecavir	Biskalcitrate	Natalizumab
Bortezomib	Vorinostat	Sorafenib
Ropinirole	Sitagliptin	Sunitinib
Remifentanyl	Ciclesonide	Dexrazoxane
Perflubutane	Telbivudine	Antithrombin alfa
Agalsidase Alfa	Kunecatechins	Sitaxentan
Laronidase	Paliperidone	Perflutren
	Alglucosidase alfa	Deferasirox
	Ranibizumab	Buprenorphine
	Idursulfase	Varenicline
	Panitumumab	Exenatide
		Dasatinib

In addition, regarding NMEs that have been approved in the last five years, we investigated the presence/absence of approvals and the times in the US and the EU, based on review reports of Japan. If the precedent approvals in other countries were described, we included those situations. Furthermore, we sought confirmation for UK medicines at the website of electronic Medicines Compendium Updates (<http://www.medicines.org.uk/mcupdates/>). In the tables, ingredients are presented using International Non-proprietary Names (INN).

3. NMEs THAT WERE APPROVED IN 2006

The numbers of NMEs that were approved in 2006 in Japan, the US and the EU (EMA) were 20, 24 and 25, respectively, showing no major differences (Table 1). Among them, there were no NMEs approved by all three regions in 2006; but entecavir was approved in both Japan and the EU, and 4 NMEs (sunitinib, varenicline, dasatinib and alglucosidase alfa) were approved in both the US and the EU.

4. ANALYSIS OF NMEs APPROVED IN MORE THAN ONE REGION AND PRECEDENT APPROVALS

Among the NMEs approved in Japan between 2002 and 2006 (including fixed combination drugs containing two NMEs), there were 70 ingredients that have been approved to date in the US or the EU; of which 69 were approved in the US, and 35 in the EU (Tables 2 and 3). On the other hand, there were 23 ingredients that were not approved in the EU but were approved in other countries including the UK. Of the 70 ingredients, only 3 received precedent approval in Japan: eletriptan, gefitinib and micafungin. The number of ingredients receiving precedent approval in the US was 57, and this included 42 ingredients that were approved before 2001. Inulin was approved in 1940 in the US and has been listed in the US Pharmacopeia, but is not sold in the US at present. Ten ingredients received precedent approval in the EU. Furthermore, there are 14 ingredients that were confirmed to have received precedent approval in countries other than the three regions: 6 ingredients in the UK, 2 each in France and Germany (among them, solifenacin was approved during the same period in both countries), and one each in Switzerland, New Zealand, Australia, the Netherlands, and Sweden.

On the other hand, there were 39 ingredients that were not approved in Japan but were approved in both the US and the EU between 2002 and 2006 (Tables 4 and 5). Of these 39 ingredients, those receiving precedent approvals numbered 28 in the US, and 11 in the EU.

Of the above 109 ingredients that were approved in two or three regions, those receiving precedent approval numbered 3 in Japan, 85 in the US, and 21 in the EU. If differences of 6 months or less in the timing of approval are regarded as simultaneous approvals, there were few simultaneously approved ingredients between Japan: 2 in 2003 in Japan and the US; and 1 in 2003, 2 in 2004, and 1 in 2006 in both Japan and the EU. On the other hand, for simultaneous approval in the US and the EU, the numbers were 6 before 2001, and then 2 in 2002, 5 in 2003, 6 in 2004, 1 in 2005, and 4 in 2006.

Table 2. NMEs approved in Japan and at least one other region (2002-2006)

NMEs	Japan	US	EU	Others*
Quinupristin/ Dalfopristin **	01/2002	09/1999	--	08/2002: UK
Infliximab	01/2002	08/1998	08/1999	--
Basiliximab	01/2002	05/1998	10/1998	--
Cladribine	01/2002	02/1993	04/2004	02/1995:UK
Risedronate	01/2002	03/1998	--	10/1999: UK
Palivizumab	01/2002	06/1998	08/1999	--
Gatifloxacin	04/2002	12/1999	--	--
Salmeterol	04/2002	02/1994	--	10/1996: UK
Eletriptan	04/2002	12/2002	--	02/2001:UK
Exemestane	07/2002	10/1999	--	12/1998: UK
Loratadine	07/2002	04/1993	--	09/2002: UK
Gefitinib	07/2002	05/2003	--	--
Esmolol	10/2002	12/1986	--	--
Ivermectin	10/2002	11/1996	--	--
Micafungin	10/2002	03/2005	--	--
Telmisartan	10/2002	11/1998	12/1998	--
Brinzolamide	10/2002	04/1998	03/2000	--
Sevelamer	01/2003	10/1998	01/2000	--
Leflunomide	04/2003	09/1998	--	07/1999: UK
Capecitabine	04/2003	04/1998	02/2001	--
Rizatriptan	07/2003	06/1998	--	06/1998: UK
Pramipexole	10/2003	07/1997	10/1997	--
Telithromycin	10/2003	04/2004	07/2001	--
Peginterferon Alfa-2a	10/2003	10/2002	6/2002	07/2001: Switzerland
Verteporfin	10/2003	04/2000	07/2000	--
Insulin glargine	10/2003	04/2000	06/2000	--
Atazanavir	12/2003	06/2003	03/2004	--
Dexmedetomidine	01/2004	12/1999	--	--
Raloxifene	01/2004	12/1997	--	07/2003: UK
Olmesartan	01/2004	04/2002	--	08/2002: Germany
Agalsidase Beta	01/2004	04/2003	--	--
Tenofovir	03/2004	10/2001	02/2002	--
Vardenafil	04/2004	08/2003	03/2003	--
Zoledronic Acid	10/2004	08/2001	04/2005	03/2003:UK
Tiotropium	10/2004	01/2004	--	05/2002:UK
Adefovir	10/2004	09/2002	03/2003	--
Peginterferon Alfa-2b	10/2004	01/2001	03/2000	--
Valganciclovir	11/2004	03/2001	--	04/2002: UK
Fosamprenavir	12/2004	10/2003	07/2004	--
Etanercept	01/2005	11/1998	02/2000	--
Rosuvastatin	01/2005	08/2003	--	03/2003:UK

NMEs	Japan	US	EU	Others*
Oxaliplatin	03/2005	08/2002	--	04/1998: France
Emtricitabine	03/2005	07/2003	10/2003	--
Bosentan	04/2005	11/2001	05/2002	--
Voriconazole	04/2005	05/2002	03/2002	--
Follitropin beta	04/2005	09/1997	05/1996	1995: New Zealand
Fludeoxyglucose(18F)	07/2005	1994	--	2002:UK
Gemtuzumab	07/2005	05/2000	--	--
Inulin	10/2005	1940	--	--
Finasteride	10/2005	06/1992	--	04/1992: Australia
Miglitol	10/2005	12/1996	--	07/1996: Netherland
Moxifloxacin	10/2005	12/1999	--	06/1999: Germany
Aripiprazole	01/2006	11/2002	06/2004	
Letrozole	01/2006	07/1997	--	11/1996:UK
Clopidogrel	01/2006	11/1997	07/1998	
Follitropin alpha	01/2006	09/1997	10/1995	
Cetorelix	04/2006	08/2000	04/1999	
Tolterodine	04/2006	05/1998	--	09/1997: Sweden
Sertraline	04/2006	12/1991	--	
Solifenacin	04/2006	12/2004	--	12/2003: Germany, France
Gabapentin	07/2006	12/1993	--	11/2005: UK
Temozolomide	07/2006	08/1999	01/1999	
Interferon bera-1a	07/2006	05/1996	03/1997	
Entecavir	07/2006	03/2005	06/2006	
Bortezomib	10/2006	05/2003	04/2004	
Ropinirole	10/2006	09/1997	--	07/1996:UK
Remifentanil	10/2006	07/1996	--	10/1996:UK
Agalsidase alfa	10/2006	--	08/2001	
Laronidase	10/2006	04/2003	06/2003	

* Except for the drugs approved through EMEA centralized procedures.

** Combination drug.

Table 3. Number of approval and preceding drugs in Japan and other regions*

	Number of approval	Number of preceding drugs
Japan	70	3
US	69	57
EU	35	10

* Number of preceding drugs and NMEs approved in Japan and at least one other region in 2002 to 2006.

Table 4. NMEs approved solely in US and EU (2002-2006)

NMEs	US	EU
Nitisinone	01/2002	02/2005
Fulvestrant	04/2002	03/2004
Oxybate	07/2002	10/2005
Pegvisomant	03/2003	11/2002
Enfuvirtide	03/2003	05/2003
Aprepitant	03/2003	11/2003
Miglustat	07/2003	11/2002
Palonosetron	07/2003	03/2005
Daptomycin	09/2003	01/2006
Memantine	10/2003	05/2002
Tadalafil	11/2003	11/2002
Bevacizumab	02/2004	01/2005
Cetuximab	02/2004	06/2004
Pemetrexed	02/2004	09/2004
Cinacalcet	03/2004	10/2004
Insulin glulisine	04/2004	09/2004
Duloxetine	08/2004	12/2004
Erlotinib	11/2004	09/2005
Natalizumab	11/2004	06/2006
Iloprost	12/2004	09/2003
Pregabalin	12/2004	07/2004
Darifenacine	12/2004	10/2004
Ziconotide	12/2004	02/2005
Palifermin	12/2004	10/2005
Pegaptanib	12/2004	01/2006
Clofarabine	12/2004	05/2006
Exenatide	04/2005	11/2006
Galsulfase	05/2005	01/2006
Insulin Detemir	06/2005	06/2004
Tripranavir	06/2005	10/2005
Tigecycline	06/2005	04/2006
Deferasirox	11/2005	08/2006
Sorafenib	12/2005	07/2006
Sunitinib	01/2006	07/2006
Alglucosidase alpha	04/2006	03/2006
Rasagiline	05/2006	02/2005
Varenicline	05/2006	09/2006
Dasatinib	06/2006	11/2006
Posaconazole	09/2006	10/2005

Table 5. Number of approval and preceding drugs in US and EU*

Year of approval	Number of approval in US	US preceding	EU preceding
2002	3	3	0
2003	8	4	4
2004	15	12	3
2005	7	6	1
2006	6	3	3
Total	39	28	11

* Number of preceding drugs and NMEs approved solely in US and EU (2002-2006).

CONCLUSION

For the year 2006, there were no major differences in the number of approvals among the three regions. On the other hand, the analysis of NMEs approved in the three regions between 2002 and 2006 showed that the number judged to have been simultaneously approved in both Japan and the US or the EU was only 6, in contrast to 18 ingredients approved in both the US and the EU. In this study, the evaluation for the EU included only those ingredients approved by the Centralized Approval Process by the EMEA, and hence did not include individual ingredients approved by each country's government or by the Mutual Recognition Procedure in the EU region. As a consequence, the number of approved ingredients may have been reduced; though new ingredients that have already been used in the EU region but approved for the first time by the EMEA for brand new indications such as orphans may have been counted in the annual number of approvals. In the investigation performed previously to review the period between 2000 and August 2004 [1], it was shown that among 105 ingredients approved in the US, the average review periods for 21 ingredients approved in both Japan and the US were 18.2 months and 19.0 months, respectively, not significantly different, despite 82 ingredients were not approved in Japan at that time. This result may suggest that there are many cases in which a drug marketed in Western countries is introduced to Japan after effectiveness, safety have been confirmed. In the US, as the review system has been strengthened by the Prescription Drug User Fee Act, new drugs have received precedent approval, thereby allowing the public to benefit from the newest medical advances [2]. However, it has been pointed out that people are initially exposed to risks, and this analysis also confirmed that observation. In Japan, there is increasing concern about promptly providing necessary drugs to clinical practitioners in terms of enhancing both medical care and economy. Japan established the Pharmaceuticals and Medical Devices Agency in 2004 to strength the review system. Furthermore, numerous proposals have been made regarding strengthening of the review system and expediting the review process in the "New Health Frontier Strategy (Eminent Persons Meeting on New Health Frontier Strategy, April 18, 2007)," the "5-Year Strategy for Innovative Pharmaceuticals and Medical Devices Creation (Ministry of Education, Culture, Sports, Science and Technology; Ministry of Health, Labour and Welfare; and Ministry of Economy, Trade and Industry, April 26, 2007)", Innovation 25 (promulgated at a Cabinet meeting, June 01, 2007), the Basic Policies for Economic and Fiscal Reform 2007 (Council on Economic and Fiscal Policy, June 19, 2007),

The Report of the Study Group on promptly providing safe and effective drugs (Ministry of Health, Labor and Welfare, July 27, 2007) , etc. However, we must consider not only the review time, but also the necessity of striving for promotion of development stages leading up to the approval application that involves improving the environments of clinical studies designed to promote participation and competition in simultaneous global developments.

REFERENCES

- [1] Saito M, Hirata-Koizumi M, Miyake S, Hasegawa R. Comparison of approval times for new prescription drugs in Japan and USA. *Proceedings of the 125th Annual Meeting of the Pharmaceutical Society of Japan*, 4,218 (2005).
- [2] Berndt ER, Gottschalk AH, Philipson TJ, Strobeck MW., Industry funding of the FDA: effects of PDUFA on approval times and withdrawal rates. *Nat Rev Drug Discov.*, 4, 545-554 (2005).

病院情報システムを用いた医療用医薬品による副作用の検出に関するパイロット研究

頭金 正博[#], 齋藤 充生, 石黒昭博^{*1}, 三宅真二, 鈴木美和子^{*2}, 折井孝男^{*2}, 長谷川 隆一

Pilot Study of Data Collection System for Adverse Reactions of Prescribed Medications using Hospital Information Systems

Masahiro Tohkin[#], Mitsuo Saito, Akihiro Ishiguro^{*1}, Shinji Miyake, Miwako Suzuki^{*2}, Takao Orii^{*2}, Ryuichi Hasegawa

We attempted to establish an efficient information data collection system for very low frequent adverse drug reactions using a hospital information system. We collected the prescription data of all patients treated with statins at the Kanto Hospital from the drug order system. At the same time, we surveyed the laboratory data on rhabdomyolysis (creatine kinase) and kidney functions (creatinine and blood and urine nitrogen) of all the patients from examination order system. Thereafter, we collated the prescription data and the laboratory data to prepare a time-series table of medications and laboratory data for each patient. We extracted patients who showed abnormal increase of the serum creatine kinase from the time-series tables and analyzed the correlations between the increase in the serum creatine kinase and the dosage, kidney functions, age, or gender. From these results, we concluded that this information data collection system was useful for the post-marketing surveys of the incidence of adverse reactions occurring at a very low frequency.

Keywords: adverse drug reactions, hospital information system, rhabdomyolysis, statin

1. 緒言

スタチン系薬剤は高脂血症の治療薬として汎用されているが、副作用（薬剤の有害反応）として横紋筋融解症を発症する場合がある。発症頻度は極めて稀であるが、一旦発症すると副作用としては重篤であり、死亡する場合もある。しかし、スタチン系高脂血症薬による横紋筋融解症の発症機構については、ほとんど明らかにされておらず、医薬品の開発段階で横紋筋融解症の発症リスクを評価し、服用前に発症を予防することは現状では極めて困難である¹⁾。したがって、スタチン系薬剤の副作用に関するリスクを推定するためには、市販後のスタチン系高脂血症薬による横紋筋融解症の発症頻度などを正確に把握することが重要になる。しかし、横紋筋融解

症は極めて稀にしか発症しないことから、スタチン系薬剤による横紋筋融解症の発症頻度に関する正確なデータを収集するためには、数万人以上の服用患者を確保する必要があり、そのためには膨大な労力と経費や時間が必要となる。このような状況は、極めて稀にしか発生しない副作用の調査には共通した課題となっており、市販後の医薬品に対する迅速な安全対策を実施する上での問題となっていることから、迅速で安価な調査方法の開発が望まれている。

ところで、我が国における病院情報システムの普及率は年々増加しており、全国規模での調査によると、600床以上の病院を対象とした場合は、平成17年度で4分の1以上にのぼり、大規模病院での入院・外来患者数を考慮するとかなりの症例数を集めることが期待できる²⁾。病院情報システムは、各病院の医療状況に合わせて病院毎にカスタマイズしたシステムが用いられている場合が多く、その仕様や操作方法はシステムのプラットフォーム毎に異なっており、データの内容や扱い方も当然異なっているものの、我が国の医療環境や健康保険システムに適合させるために、共通な仕様となっている部分もある³⁾。そこで、病院情報システムの共通仕様機能を用い

[#] To whom correspondence should be addressed: Masahiro Tohkin; 1-18-1 Kamiyoga Setagaya-ku, Tokyo 158-8501, Japan; Tel: 03-3700-1141 ext567; Fax 03-3700-9788; E-mail: tohkin@nihs.go.jp

^{*1} (独) 医薬品医療機器総合機構安全部 (医薬安全科学部・協力研究員)

^{*2} NTT東日本 関東病院薬剤部

て、医薬品の使用状況と副作用の発生状態についての汎用性のある調査システムが構築できれば、全国を対象とした副作用調査が、比較的安価で迅速に実施できる可能性がある。

以上のような考えにもとづいて、我々はスタチン系高脂血症薬を服用している患者を対象に、病院情報システムに保存されているスタチン系高脂血症薬の使用状況と横紋筋融解症に関連した検査値および腎機能、年齢、性別などの患者背景因子を網羅的に収集し、稀にしか発症しない副作用の発症頻度や患者背景因子との関係を調査する方法を開発することを目的とし、NTT東日本関東病院（関東病院）の病院情報システムの薬剤データ等を用いてパイロット研究を行った。

2. 調査研究方法

2-1. 関東病院での調査対象

関東病院で収集された研究対象者（被験者）の処方情報と検査値情報は匿名化された後に国立医薬品食品衛生研究所・医薬安全科学部へ電子データとして提供され、横紋筋融解症に関連した解析に用いられた。

(1) 調査対象

関東病院に入院・外来のリボバス（シンバスタチン）、メバロチン（プラバスタチン）、リビトール（アトルバスタチン）、ローコール（フルバスタチン）、リバロ（ピタバスタチン）、クレストール（ロスバスタチン）のいずれかを服用している患者

(2) 調査対象期間

平成19年1月～平成19年6月

(3) 調査項目

(i) 患者背景

年齢、性別

(ii) 対象薬剤の使用状況

投与薬剤名、一日投与量、投与期間、処方せん発行日

(iii) 横紋筋融解症に関連した臨床検査値

血清クレアチンキナーゼ値 (CK)

(iv) 腎機能に関連した臨床検査値

血清クレアチニン値 (Cre)、血中尿素窒素値 (BUN)、検査実施日

(4) 同意取得について

当研究は人体から採取された試料を用いない、既存資料等のみを用いる後ろ向き観察研究であり、全ての診療情報が資料提供機関で匿名化されることから、研究対象者からは、インフォームド・コンセントの取得は行わない（疫学研究に関する倫理指針「第7項 研究対象者からインフォームド・コンセントを受ける手続き等、(2)観察研究を行う場合 ②人体から採取さ

れた試料を用いない場合」および「第11項 他の機関等の資料の利用、(2)既存資料等の提供にあたっての措置」参照)。なお、研究参加医療機関で研究対象となる可能性のある患者へは、当研究が実施されることを広報し周知させる努力を払った。また、本研究は国立医薬品食品衛生研究所・研究倫理審査委員会により、調査方法等について審査を受け実施が許可されている（受付番号145）。

2-2. 関東病院でのスタチン系高脂血症薬の服用患者における血清クレアチンキナーゼ値上昇に関する調査

関東病院の病院情報システムは、電子診療録（電子カルテ）システムを中心に、診療支援、外来、患者サービス、薬剤支援、経営管理・物流、入院の各システムが連携している。処方システムと臨床検査システムは、電子診療録（電子カルテ）システムの中のオーダリングシステムに含まれるが、各オーダリングシステムは独立している。したがって、スタチン系高脂血症薬の服用患者の使用状況、検査値、入院・外来期間等のデータを病院情報システム上で患者単位のデータとして一括して検索・抽出することはできない。そこで、それぞれのシステムのデータセットから匿名化患者記号を指標にして抽出し、マイクロソフト・エクセルでスタチン系高脂血症薬の処方オーダー情報と検査値オーダーを統合する事にした。具体的な方法はFig.1に示す手順で患者情報の抽出と統合を行った。まず、調査期間内にスタチン系高脂血症薬処方オーダー歴のある患者データを診療系オーダーシステムから抽出し、匿名化患者記号、投与回数、投与日数、処方せん発行日等のデータを抽出する。期間内に1人の患者が複数回のスタチン系高脂血症薬の処方を受けているので、匿名化患者記号を指標にしてマイクロソフト・エクセルを用いて患者一覧表を作成し、重複する匿名化患者記号を1個の記号に統合し、時系列でスタチ

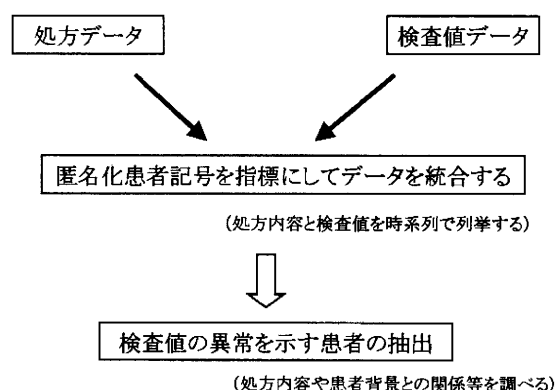


Fig. 1 Flow chart for the combination of prescription data and laboratory data

Table 1 Examples of prescription data, laboratory data, and time-series table

(A) Prescription data

薬品名	匿名化患者記号	処方日	処方量	日数
クレストール錠 2.5mg	abcdefgh	4/4	1	35
クレストール錠 2.5mg	bsdefghi	4/5	1	35
クレストール錠 2.5mg	cdefghijk	4/9	1	35
クレストール錠 2.5mg	defhijkl	4/9	1	28
クレストール錠 2.5mg	efghijklm	4/9	1	28
クレストール錠 2.5mg	fghijklmn	4/9	1	35
クレストール錠 2.5mg	ghijklmno	4/10	1	35
クレストール錠 2.5mg	hijklmnop	4/10	1	42
クレストール錠 2.5mg	ijklmnopq	4/11	1	68
クレストール錠 2.5mg	klmnopqr	4/11	1	35
クレストール錠 2.5mg	lmnopqrs	4/12	1	28
クレストール錠 2.5mg	mnopqrst	4/15	1	56
クレストール錠 2.5mg	nopqrstu	4/15	2	60
クレストール錠 2.5mg	opqrstuv	4/15	1	35
クレストール錠 2.5mg	pqrstuvw	4/16	1	56
クレストール錠 2.5mg	qrstuvwx	4/16	2	35
クレストール錠 2.5mg	rstuvwxy	4/16	1	56
クレストール錠 2.5mg	stuvwxyz	4/16	1	28
クレストール錠 2.5mg	tuvwxyzab	4/17	1	20
クレストール錠 2.5mg	vwxyzabc	4/17	1	56
クレストール錠 2.5mg	vwxyzabc	4/18	1	76

(B) Laboratory data

検査日	匿名化患者記号	検査項目	結果値
4/1	wxyzabcd	Cre	1.33
4/1	wxyzabcd	BUN	22.00
4/1	wxyzabcd	CK	47.00
4/1	zabcdefg	Cre	0.47
4/1	zabcdefg	BUN	17.80
4/1	zabcdefg	CK	30.00
4/1	abcdefgh	Cre	0.99
4/1	abcdefgh	BUN	11.50
4/1	abcdefgh	CK	44.00
4/1	bsdefghi	Cre	1.40
4/1	bsdefghi	BUN	24.30
4/1	bsdefghi	CK	13.00
4/1	cdefghijk	Cre	1.56
4/1	cdefghijk	BUN	30.40
4/1	cdefghijk	CK	477.00
4/1	defhijkl	Cre	0.54
4/1	defhijkl	BUN	7.50
4/1	defhijkl	CK	58.00
4/1	efghijkl	Cre	0.80
4/1	efghijkl	BUN	20.50

(C) Time-series table of medications and laboratory data for each patient

	処方日	1/10	2/14	3/14	4/17	5/15	6/12	検査日	2/14	3/14				
		処方量	1	1	1	1	1	1	CK	81.00	76.00			
日数	35	28	28	28	28	28	CK	0.69	0.70					
							BUN	11.60	15.00					
bsdefghi	処方日	1/16	3/6	6/12				検査日	1/16	3/6	6/12			
	処方量	1	1	1				CK	164.00	142.00	177.00			
	日数	56	98	98				CK	0.56	0.58	0.61			
							BUN	18.20	14.90	17.20				
cdefghijk	処方日	6/15						検査日	1/5	1/5	2/13	2/13	4/13	6/15
	処方量	1						CK	157.00	158.00	167.00	180.00	355.00	191.00
	日数	56						CK	0.83	0.83	0.87	0.87	0.86	0.90
							BUN	25.90	26.50	18.90	19.50	20.50	15.30	
defhijkl	処方日	1/9						検査日	1/9	2/13	3/13	4/24	5/29	
	処方量	1	1	1	1	1		CK	152.00	148.00	80.00	142.00	247.00	
	日数	35	28	42	35	28		CK	2.00	2.34	1.90	2.01	2.11	
							BUN	43.60	36.30	31.10	37.00	51.70		
efghijklm	処方日	1/15						検査日	1/15					
	処方量	1	1	1				CK	132.00					
	日数	56	90	97				CK	1.04					
							BUN	14.80						
fghijklmn	処方日	2/27						検査日	2/27	5/28				
	処方量	1	1					CK	70.00	73.00				
	日数	90	98					CK	0.91	1.04				
							BUN	15.50	24.00					
ghijklmno	処方日	1/23						検査日	1/23	2/27	3/27	5/1		
	処方量	1	1	1	1			CK	Blank	122.00	157.00	144.00		
	日数	35	28	35	35			CK	0.67	0.68	0.70	0.69		
							BUN	Blank	14.10	14.20	11.70			

ン系高脂血症薬の処方状況を整理した (Table 1 (A)). 一方, 検査系オーダーシステムから調査期間内の全ての患者についての今回の調査に必要な, CKやBUN, Cre等の臨床検査値を全て抽出し, 臨床検査値一覧表を作成した (Table 1 (B)). マイクロソフト・エクセルを用いて, スタチン系高脂血症薬の服用患者一覧表と臨床検査値一覧表を統合し, 患者毎のスタチン系高脂血症薬の投与状況と検査値の変動を時系列で表示した (Table 1 (C)).

2-3. 全国規模でのスタチン系高脂血症薬の使用実態調査

日本病院薬剤師会が実施した調査で病院情報システムを導入していると報告した医療機関のうち300床以上の医療機関 (204施設) を対象にして, 平成17年度のスタチン系高脂血症薬の処方数をアンケート方式で調べ集計した.

3. 調査結果

3-1. スタチン系高脂血症薬の使用実態

関東病院の全ての入院・外来患者のうち平成19年1月~平成19年6月までの6ヶ月間でスタチン系高脂血症薬を投与された患者の総数は4,086名であった. 各スタチン系高脂血症薬の使用患者数ではリピトールがもっとも多く, ついで, メバロチンが多く処方されていた (Table 2). 一方, ローコールの処方患者数は少なく73名のみであった. 使用薬剤構成比について, 平成17年度に実施した全国の204施設を対象とした調査結果 (Fig. 2) と比較すると, 関東病院での使用状況はリピトールの使用量が比較的多い点とローコールの使用量が少ない点が全国的な平均と異なっていた. 関東病院での Crestor

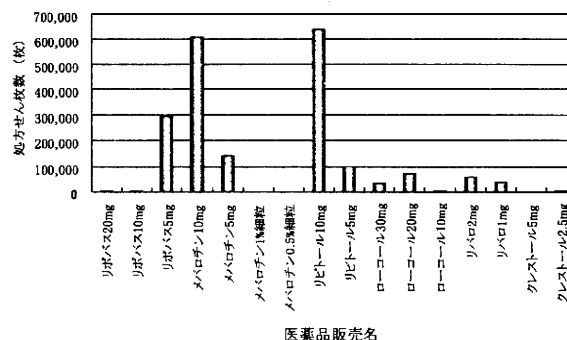


Fig. 2 Number of prescriptions for statins in the nation-wide 204 medical institutions

の使用量が多いのは調査年の影響と思われる.

3-2. 血清クレアチンキナーゼ値異常患者の頻度

スタチン系高脂血症薬服用患者4086名のうち, 血清クレアチンキナーゼ (CK) 値が500 IU/L以上の高値を示す患者は122名であった (Table 2). また, 薬剤毎のCK値が高値の患者数を集計したところ, 今回調査した中では, クレストール, ローコール, リバロの頻度が高かった (Table 2).

次に, 各製薬企業が市販後等に調査したCK値の異常の頻度について, 添付文書やインタビューフォームに記載している数字を調査し, Table 3にまとめた. また, 関東病院で調査したCK高値 (500 IU以上) の頻度と, 添付文書等に記載されていた頻度をFig. 3に示した. その結果, 今回の調査から得られた頻度の数字は添付文書に記載されている数字の2~3倍程度であったが, 各薬剤での頻度の順はリピトールを除いて添付文書でのCK上昇の順と一致した. リピトールの添付文書に記載されている頻度については, 調査母数が他の薬剤に比べて少

Table 2 Number of patients showing high values of creatine kinase and kidney function

医薬品販売名	患者総数 (人)	CK上昇*		腎機能検査値異常				CK&腎機能 検査値異常‡	
		(人)	(%)	Cre上昇**		BUN上昇†		(人)	(%)
クレストール	207	9	4.3	27	13	52	25.1	6	2.9
ローコール	73	3	4.1	3	4.1	13	17.8	0	0.0
リバロ	288	12	4.2	32	11	61	21	8	3
リピトール	2118	71	3.4	244	12	512	24	43	2
リポバス	431	10	2.3	37	9	96	22	4	1
メバロチン	969	17	1.8	97	10	206	21	10	1
合計	4086	122	-	440	-	940	-	71	-
平均	-	-	3.3	-	9.7	-	22	-	1.6

* CK値が500 IU/L以上の示す患者
 ** Cre値が1.2 mg/dL以上の示す患者
 † BUN値が20 mg/dL以上の示す患者
 ‡ CK上昇症例のうちCreもしくはBUNも上昇した症例

Table 3 Information of creatine kinase and kidney function, which are described in the package inserts of statins

#	医薬品販売名	CK値上昇	Cre値上昇	BUN値上昇
1	Crestor	国内・外の臨床試験(承認時):1.6%(171/10380例) 使用成績調査(2007年2月報告時):2.3%(201/8795例)	記載なし	記載なし
2	Loxol	カプセル剤の承認時まで及び市販後2002年2月までの集計:1.5%(93/6368例)	0.1~5%未満	0.1~5%未満
3	Ripabro	0.1%~2.0% ※インタビューフォーム:1.6%(323/20888例)	0.1%未満	0.1%未満
4	Ripitor	5%以上 ※インタビューフォーム:6%(54/893例)	記載なし	頻度不明
5	Ripovas	治験(2.5~10mg/日投与):4.2%(42/1002例) 用量拡大治験(5~20mg/日投与):5.5%(29/531例) 使用成績調査(第4年次迄の累計:5~10mg/日投与):0.8%(65/8123例)	記載なし	0.1~5%未満
6	Mevalochin	0.1~1%未満 ※インタビューフォーム:0.5%(61/11137例)	0.1%未満	0.1%未満

特記ない場合、「その他の副作用」の項において記載されている頻度に関する情報を示す

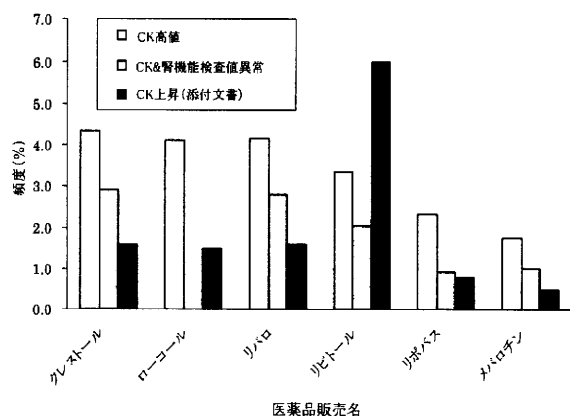


Fig. 3 Frequencies of patients showing high values of creatine kinase and abnormal kidney function

Frequencies of patients who showed high values of creatine kinase and abnormal kidney function are cited from this survey results and from package insert of statins

ないことから、市販後調査ではなく、治験のデータである可能性がある (Table 3)。

3-3. 血清クレアチンキナーゼ高値と患者背景要因との関係

CK 値の上昇と患者側の要因との関係を調べるため、スタチン系高脂血症薬の投与量および投与患者の腎機能を調べた。投与量については、Table 4 に示したように、同じスタチン系高脂血症薬での異なる投与量とCK 上昇患者数の関係を調べたところ、CK 値が高値を示す以前の投与量のデータが今回の調査期間に含まれないために、投与量を特定できない場合が多かったが、投与量が特定可能であった症例では、投与量が多い場合でも必ずしもCK 上昇患者数が多いとはいえなかった。また、腎機能との関係を調べるために、CK 上昇患者での

Table 4 Dosage of statins in patients showing high values of creatine kinase

医薬品販売名	投与量 (CK値:>500発現時)				
	患者数				
Crestor 錠	2.5mg		不明*		
	3		6		
Loxol 錠	30mg		不明*		
	3		0		
Ripabro 錠	1mg	2mg	4mg	不明*	
	1	1	2	8	
	Ripitor 錠			不明*	
	5mg	10mg	20mg	37	
Ripovas 錠	5mg	10mg	不明*		0
	7	3			
	Mevalochin 錠				
5mg	10mg	20mg	40mg	不明*	
2	4	1	1	9	

不明*は調査開始時に既にCK値が高値を示していたため、投与量を特定できなかった

血清クレアチニン値 (Cr) と血清尿素窒素 (BUN) を測定し、基準値 (Cr>1.2 あるいはBUN>20) 以上を示す腎機能が低下した患者数を集計し頻度を計算した (Table 2)。CK 値が高値を示す患者のうち腎機能が低下した患者数についても集計した (Table 2)。その結果、薬剤によってはCK 高値患者の中に腎機能の低下している患者が高い割合で含まれている場合もあったが、今回の調査の範囲では腎機能が低下した時期とCK 値が上昇した時期の関係が必ずしも明確でなく、腎機能とCK 上昇との明確な関係は不明であった。

スタチン系高脂血症薬の投与患者のうち、65歳以上の患者のみを高年齢患者群として抽出しCK 値および腎機能検査値を集計したところ、高年齢患者群では腎機能の低下を示す患者の割合はスタチン系高脂血症薬の投与患

者全体に比べて増加しているものの、CK値の高値を示す患者割合は全体と差はなかった (Table 5)。また、投与患者を性別で集計した場合は、腎機能の低下を示す患者の割合は男女で差はなかったが、CK値の高値を示す患者の割合は男性の方が多かった (Table 6)。

4. 考察

本研究ではパイロット研究として、関東病院における病院情報システムのデータソースから、匿名化患者記号を指標とし、スタチン系高脂血症薬の使用患者と臨床検査データを汎用ソフトであるマイクロソフト・エクセル

Table 5 Number of elderly patients showing high values of creatine kinase and abnormal kidney function

65歳以上 (高齢者)

医薬品販売名	患者総数 (人)	CK上昇*		腎機能検査値異常				CK&腎機能 検査値異常‡	
				Cre上昇**		BUN上昇†			
				(人)	(%)	(人)	(%)		
Crestol	70	4	5.7	18	25.7	29	41.4	3	4.3
ローコール	42	1	2.4	2	4.8	9	21.4	0	0.0
リバロ	138	6	4.3	26	19	44	32	6	4
リピトール	1151	37	3.2	171	15	370	32	31	3
リポバス	298	5	1.7	28	9.4	73	24.5	2	0.7
メバロチン	620	10	1.6	78	13	165	27	7	1
合計	2319	63	-	323	-	690	-	49	-
平均	-	-	2.9	-	14.4	-	29.2	-	2.2

* CK値が500 IU/L以上の示す患者

** Cre値が1.2 mg/dL以上の示す患者

† BUN値が20 mg/dL以上の示す患者

‡ CK上昇症例のうちCreもしくはBUNも上昇した症例

Table 6 Number of patients showing high values of creatine kinase and abnormal kidney function in each gender

男性

医薬品販売名	患者総数 (人)	CK上昇*		腎機能検査値異常				CK&腎機能 検査値異常‡	
				Cre上昇**		BUN上昇†			
				(人)	(%)	(人)	(%)		
Crestol	106	7	6.6	17	16.0	24	22.6	5	4.7
ローコール	42	2	4.8	2	4.8	7	16.7	0	0.0
リバロ	186	9	4.8	29	16	44	24	6	3
リピトール	1355	55	4.1	189	14	326	24	30	2
リポバス	217	7	3.2	30	13.8	56	25.8	4	1.8
メバロチン	468	10	2.1	67	14	108	23	5	1
合計	2374	90	-	334	-	565	-	50	-
平均	-	-	3.8	-	13.4	-	22.4	-	2.2

女性

医薬品販売名	患者総数 (人)	CK上昇*		腎機能検査値異常				CK&腎機能 検査値異常‡	
				Cre上昇**		BUN上昇†			
				(人)	(%)	(人)	(%)		
Crestol	101	2	2.0	10	9.9	28	27.7	1	1.0
ローコール	31	1	3.2	1	3.2	6	19.4	0	0.0
リバロ	102	3	2.9	3	3	17	17	2	2
リピトール	763	16	2.1	55	7	186	24	13	2
リポバス	214	3	1.4	7	3.3	40	18.7	0	0.0
メバロチン	501	7	1.4	50	6	98	20	5	1
合計	1712	32	-	106	-	375	-	21	-
平均	-	-	2.1	-	5.3	-	20.4	-	0.9

* CK値が500 IU/L以上の示す患者

** Cre値が1.2 mg/dL以上の示す患者

† BUN値が20 mg/dL以上の示す患者

‡ CK上昇症例のうちCreもしくはBUNも上昇した症例

を用いて統合し、全てのスタチン系高脂血症薬の服用患者から横紋筋融解症のマーカーであるCK値が高値を示す患者を抽出し、薬剤毎のCK上昇の患者発症頻度を算出することが可能であることを示した。今回の調査から算出した発症頻度と添付文書に記載されているCK値の上昇の頻度については、各薬剤間の相対的な傾向はほぼ一致していた。したがって、我々の考案した病院情報システムを使用した医薬品の使用状況と副作用の発生状態についての調査システムについては、病院情報システムのプラットフォームが異なっても実施可能であり、算出した発症頻度についてもほぼ満足できる数字であることが明らかになった。市販後の医薬品における副作用の調査としては、薬事法に基づく副作用報告のデータを用いた調査がある。副作用報告に基づくデータは全ての市販されている医薬品を対象にしている点や全国を網羅している点で優れたデータであるものの、使用者総数は集計されていないため頻度を算出することができない。その他にも、製薬企業が実施する市販後調査があり、データの正確性などで優れているが、実施される品目が限られている点や、公表されるまでに時間がかかり経過するなどの点で問題がある。また、諸外国で行われる健康保険データを用いる調査などがあるが、我が国では今のところ健康保険データは公開されていない。以上の調査方法に比べて、我々の考案した調査方法は、病院情報システムを稼働させている病院の協力が得られれば、データの正確性、経費、調査期間のいずれにおいても優れた方法であると考えられる。

スタチン系高脂血症薬の服用患者でのCK値の上昇と患者背景要因との関係を調べるために、スタチン系高脂血症薬の投与量と患者の腎機能との関係を精査した。CK値が高値を示す以前の投与量と腎機能のデータが今回の調査期間に含まれないために投与量を特定できない場合があったが、CK値が高値を示した時期での投与量や腎機能が特定可能であった症例では、今回の調査の範囲では、両者ともCK値上昇との明確な関係は不明であった。患者の生理機能との関係を調べる場合は、CK値上昇との時期的な関係を長期間に渡って明らかにすることが必要であると思われた。また、他病院からの紹介を受けた患者などで初診時に既にCK値が高値を示した場合などは、背景因子との関係を検討する対象としては適さないと考えられた。

今回調査対象としたスタチン系高脂血症薬のほとんどの添付文書には「高齢者で横紋筋融解症があらわれやすいとの報告がある」と記載されていることから、65歳以上の患者と全体と比較したところ、既に文献で報告されているように腎機能は高齢者患者群で低下していたが⁴⁾、CK値の高値を示す患者の割合は全体と差はなかったこ

とから、添付文書の記載については今回の結果から確認することはできなかった。また、男女でのCK値の高値を示す患者の割合を比較したところ、男性の方が高い頻度を示した。この結果から男性が筋障害を生じやすい可能性が考えられたが、男性のCK値の基準値が女性より高いことを反映している可能性も考えられた。

今回の調査は1施設でのデータを用いているために、一部のスタチン系高脂血症薬の使用状況が全国的レベルでのデータと異なっていたことや、入院・外来患者の特徴に偏りがある可能性があることから、横紋筋融解症やCK高値の発症頻度などは、今回の結果を単純に一般化することはできない。しかし、全国の医療機関をこの調査の対象にすることが可能であれば、薬剤毎の副作用の発生頻度のみならず、発症患者の背景因子との関係を解析することが可能になり、医薬品の市販後安全対策にとって、貴重なデータが得られるものとする。

謝 辞

本研究を実施するに当たりましてご協力いただきました(社)日本病院薬剤師会に深謝いたします。

参考文献

- 1) 横紋筋融解症. 重篤副作用疾患別対応マニュアル 第1集, 日本医薬情報センター 2007年.
- 2) 厚生労働省大臣官房統計情報部. 平成17年患者調査.
- 3) 医療マネジメント学会: 電子カルテシステムの普及に向けて, じほう 2004年.
- 4) 加藤隆一: 薬の体内動態と年齢, 臨床薬物動態学, 南江堂 1998年.

Physiologically Based Pharmacokinetic Modeling to Predict Transporter-Mediated Clearance and Distribution of Pravastatin in Humans

Takao Watanabe, Hiroyuki Kusuhara, Kazuya Maeda, Yoshihisa Shitara, and Yuichi Sugiyama

Department of Molecular Pharmacokinetics, Graduate School of Pharmaceutical Sciences, The University of Tokyo, Tokyo, Japan (T.W., H.K., K.M., Y.S.); and Department of Biopharmaceutics, Graduate School of Pharmaceutical Sciences, Chiba University, Chiba, Japan (Y.Sh.)

Received September 25, 2008; accepted November 7, 2008

ABSTRACT

Hepatobiliary excretion mediated by transporters, organic anion-transporting polypeptide (OATP) 1B1 and multidrug resistance-associated protein (MRP) 2, is the major elimination pathway of an HMG-CoA reductase inhibitor, pravastatin. The present study examined the effects of changes in the transporter activities on the systemic and liver exposure of pravastatin using a physiologically based pharmacokinetic model. Scaling factors, determined by comparing *in vivo* and *in vitro* parameters of pravastatin in rats for the hepatic uptake and canalicular efflux, were obtained. The simulated plasma and liver concentrations and biliary excretion profiles were very close to the observed data in rats under linear and nonlinear conditions. *In vitro* parameters, determined in human cryopreserved hepatocytes and canalicular membrane vesicles, were extrapolated to *in vivo* parameters using the scaling factors

obtained in rats. The simulated plasma concentrations of pravastatin were close to the reported values in humans. Sensitivity analyses showed that changes in the hepatic uptake ability altered the plasma concentration of pravastatin markedly but had a minimal effect on the liver concentration, whereas changes in the ability of canalicular efflux altered the liver concentration of pravastatin markedly but had a small effect on the plasma concentration. In conclusion, the model allows the prediction of the disposition of pravastatin in humans. The present study suggests that changes in the OATP1B1 activities may have a small and a large impact on the therapeutic efficacy and side effect (myopathy) of pravastatin, respectively, whereas those in the MRP2 activities may have opposite impacts (i.e., large and small impacts on the therapeutic efficacy and side effect).

Predicting the disposition of drugs in humans, particularly in the early stages of drug development, has been a critical issue in selecting the proper candidate drugs because the exposure of drugs to target organs is the major factor determining their pharmacological and/or toxicological activity. Human liver microsomes allow the reliable prediction of the metabolic clearance of drugs in humans (Rane et al., 1977; Iwatsubo et al., 1997; Obach, 1999; Naritomi et al., 2001). Biliary excretion, another hepatic elimination pathway, is the major systemic elimination pathway, particularly for amphipathic anionic drugs such as HMG-CoA reductase inhib-

itors (statins) and angiotensin II receptor antagonists. Because multiple transporters on the sinusoidal and canalicular membranes are involved, it is necessary to separately determine three kinetic parameters: 1) uptake, 2) sinusoidal efflux, and 3) canalicular efflux, to predict biliary clearance with regard to the plasma concentration (Giacomini and Sugiyama, 2005; Shitara et al., 2006a). The uptake clearance determined in freshly isolated rat hepatocytes correlates well with that determined with the multiple indicator dilution method (Miyachi et al., 1993), and rat hepatocytes are reported to be a useful tool for predicting the hepatic clearance of drugs with significant hepatic uptake (Soars et al., 2007). Although cryopreserved human hepatocytes and canalicular membrane vesicles (CMVs) are commercially available, their usefulness in predicting *in vivo* hepatic up-

Article, publication date, and citation information can be found at <http://jpet.aspetjournals.org>.
doi:10.1124/jpet.108.146647.

ABBREVIATIONS: CMV, canalicular membrane vesicle; PBPK, physiologically based pharmacokinetic; OATP, organic anion-transporting polypeptide; MRP, multidrug resistance-associated protein; SF, scaling factor; R-122798, (3R,5R)-3,5-dihydroxy-7-[(1S,2S,6S,8S,8aR)-6-hydroxy-8-(isobutyryloxy)-2-methyl-1,2,6,7,8,8a-hexahydronaphthalen-1-yl]heptanoic acid; LC/MS, liquid chromatography/mass spectrometry; PS, permeability surface product; inf, influx; dif, diffusion; CL, clearance; met, metabolism; tot, total; B, blood; AUC, area(s) under the concentration-time curve.

take and canalicular efflux clearance remains to be examined. No method to quantify *in vitro* sinusoidal efflux has yet been established.

A physiologically based pharmacokinetic (PBPK) model, in which compartments representing tissues are connected with the blood flow, has been used to predict the time profiles of plasma and tissue concentrations (Kawai et al., 1998; Jones et al., 2006). The PBPK model is quite useful for simulating the effects of drug-drug interactions and genetic variations in drug-metabolizing enzymes and transporters on the exposure of drugs to the blood and organs and, ultimately, their effects on the pharmacological actions of drugs (Jones et al., 2006; Shitara and Sugiyama, 2006a). The purpose of this study was to establish a PBPK model to describe the disposition of pravastatin for which transporters are deeply involved in its hepatobiliary transport. Pravastatin, one of the statins used for the treatment of hyperlipidemia, was selected as the model compound in this study. The liver is a target organ for the pharmacological actions of statins, whereas myotoxic adverse effects, sometimes severe, including myopathy or rhabdomyolysis, are associated with the use of statins. Therefore, it is very important to simulate the exposure of statins to the liver and skeletal muscle to predict their pharmacological and toxicological effects. Hepatobiliary transport is the main elimination pathway of pravastatin from the systemic circulation and is mediated by uptake and efflux transporters in the liver (Shitara and Sugiyama, 2006b). The hepatic uptake of pravastatin is mainly mediated by organic anion-transporting polypeptide (OATP) 1B1, and its biliary excretion is predominantly mediated by multidrug resistance-associated protein (MRP) 2 (Yamazaki et al., 1993, 1997; Nakai et al., 2001). Pravastatin undergoes urinary excretion by tubular secretion and by glomerular filtration in humans (Singhvi et al., 1990). Organic anion transporter 3 has been suggested to be responsible for the basolateral uptake of pravastatin in rats and humans (Hasegawa et al., 2002; Nakagomi-Hagihara et al., 2007), whereas the transporter involved in its luminal efflux is yet to be identified.

In this study, *in vivo* experiments were carried out using male rats to obtain concentration-time profiles of pravastatin in the plasma, liver, kidney, muscle, brain, and lung. The kinetic parameters for the hepatic uptake and canalicular efflux of pravastatin were determined from *in vitro* transport studies using freshly isolated rat hepatocytes and CMVs, respectively. *In vitro-in vivo* scaling factors (SFs) were obtained for the hepatic uptake and subsequent canalicular efflux of pravastatin in rats. A PBPK model was constructed to simulate the systemic and liver exposure of pravastatin in rats. Using the PBPK model, the SFs determined in rats and kinetic parameters determined using human materials, the plasma concentration-time curve of pravastatin in humans was also simulated. Finally, the effects of changes in these transporter activities, caused by genetic polymorphisms and drug-drug interactions, on the concentration profiles of pravastatin in plasma and the liver were examined using the PBPK model.

Materials and Methods

Materials

[³H]Pravastatin (45.5 Ci/mmol), unlabeled pravastatin, and a pravastatin analog, R-122798, were provided by Daiichi Sankyo Co.,

Ltd. (Tokyo, Japan). Cryopreserved human hepatocytes and human liver S9 fractions were purchased from In Vitro Technologies (Baltimore, MD). Human liver S9 fractions were also purchased from XenoTech, LLC (Lenexa, KS) and Tissue Transformation Technology (Edison, NJ). All other chemicals and reagents were of analytical grade and were readily available from commercial sources.

Animals

Male Sprague-Dawley rats (6–7 weeks old) were purchased from Nippon SLC (Hamamatsu, Japan). All animals were maintained under standard conditions with a reversed light/dark cycle and were treated humanely. Food and water were available *ad libitum*. The studies were carried out in accordance with the guidelines of the Institutional Animal Care Committee, Graduate School of Pharmaceutical Sciences, The University of Tokyo, Tokyo, Japan.

Animal Experiments

Male Sprague-Dawley rats, weighing approximately 250 to 320 g, were used throughout the experiments. Under ether anesthesia, the femoral artery was cannulated with a polyethylene catheter (SP-31) for the collection of blood samples. The bile duct was cannulated with a polyethylene catheter (PE-10) for bile collection, and the bladder was cannulated with a silicon catheter to collect urine. The femoral vein or the duodenum was cannulated with a polyethylene catheter (SP-31) for the administration of pravastatin. Each rat was placed in a Bollman cage and allowed to recover from the anesthesia before the experiments were continued. The rats were given pravastatin intravenously at 0.2, 1, 10, 50, or 200 mg/kg or intraduodenally at 20 mg/kg. Blood samples were collected at the designated times and centrifuged at 1500g for 10 min at 4°C to obtain plasma. Bile and urine samples were collected in preweighed test tubes at the designated intervals throughout the experiment. After the last blood sample had been taken, each rat was killed, and the liver, kidney, brain, lungs, and skeletal muscle were excised immediately for the tissue distribution study. The tissues were weighed and flash frozen in liquid nitrogen. All the samples were stored at –20°C until quantification.

Transport Study Using Human Cryopreserved Hepatocytes

This experiment was performed as described previously (Shitara et al., 2003). In brief, immediately before the study, the hepatocytes were thawed at 37°C. After they had been washed twice with ice-cold Krebs-Henseleit buffer, the cells were resuspended in Krebs-Henseleit buffer to a cell density of 1.0×10^6 viable cells/ml for the uptake study. After preincubation of the cells (1.2×10^5 cells/reaction) at 37°C for 3 min, drug uptake was initiated by the addition of labeled and unlabeled substrates to the cell suspension. The reaction was terminated after 0.5 or 2 min by separating the cells from the substrate solution. For this purpose, an aliquot of 100 μ l of incubation mixture was placed in a centrifuge tube (450 μ l) containing 50 μ l of 2 N NaOH under a layer of 100 μ l of oil (density = 1.015, a mixture of silicone oil and mineral oil; Sigma-Aldrich, St. Louis, MO). The sample tube was centrifuged for 10 s in a tabletop centrifuge (10,000g; Beckman Microfuge E; Beckman Coulter, Fullerton, CA). After overnight incubation in alkali to dissolve the hepatocytes, the centrifuge tube was cut, and each phase was transferred to a scintillation vial. The phase containing the dissolved cells was neutralized with 50 μ l of 2 N HCl, mixed with scintillation cocktail, and its radioactivity was measured in a liquid scintillation counter (LS6000SE; Beckman Coulter). The time course for the uptake of [³H]pravastatin into hepatocytes was expressed as the uptake volume (microliters per 10^6 viable cells) of the radioactivity taken up into the cells (disintegrations per minute per 10^6 cells) divided by the concentration of radioactivity in the incubation buffer (disintegrations per minute per microliter). The initial uptake velocity of [³H]pravastatin was calculated from the slopes of the uptake volume versus time plots

obtained at 0.5 and 2 min and expressed as the uptake clearance (microliters per minute per 10^6 cells).

Metabolism Study Using the Liver S9 Fraction

It has been reported that pravastatin is metabolized by sulfotransferase in male rats (Kitazawa et al., 1993). Therefore, we used the liver S9 fraction as the enzyme source. The liver S9 fraction was prepared from four rats using standard procedures and stored at -80°C until use. The protein concentration was determined by the Lowry method, using bovine serum albumin as the standard. Pravastatin was incubated with a reaction mixture consisting of rat liver S9 fraction (final concentration, 8 mg/ml), NADPH-generating system (0.8 mM NADP⁺, 8 mM glucose 6-phosphate, 1 U/ml glucose-6-phosphate dehydrogenase, and 3 mM MgCl₂), and 3'-phosphoadenosine 5'-phosphosulfate (final concentrations, 0.5 and 5 mM for low and high pravastatin concentrations, respectively) in the presence of 100 mM phosphate buffer, pH 7.4. After preincubation at 37°C for 10 min, pravastatin (final concentration, 0.1–500 μM) was added to initiate the enzyme reaction. At the designated time, the reactions were terminated by mixing them with equal volumes of methanol containing R-122798, an analytical internal standard, followed by centrifugation at 15,000g for 10 min at 4°C . The supernatant was subjected to liquid chromatography/mass spectrometry (LC/MS) analysis. In studies with the human liver S9 fraction, the concentrations of pravastatin and 3'-phosphoadenosine 5'-phosphosulfate were 5 μM and 1 mM, respectively; other incubation conditions were the same as in the rat studies.

LC/MS Analysis

Liver, kidney, brain, lung, and skeletal muscle were added to 3 to 5 volumes of physiological saline (w/v) and homogenized. Tissue homogenates and plasma, bile, and urine samples were deproteinated with 2 volumes of methanol containing the internal standard (1 $\mu\text{g/ml}$ R-122798) and centrifuged at 15,000g for 10 min at 4°C . High-concentration samples were diluted appropriately with blank matrix before deproteination. The supernatant was subjected to LC/MS analysis. The appropriate standard curves were prepared in the equivalent blank matrix and used for each analysis.

The LC/MS consisted of an Alliance HT 2695 separation module with an autosampler (Waters, Milford, MA) and a Micromass ZQ mass spectrometer with an electron ion spray interface (Waters). The optimum operating conditions used were as follows: electrospray probe (capillary) voltage, 3.2 kV; sample cone voltage, 20 V; and source temperature, 100°C . The spectrometer was operated at a drying desolvation gas flow rate of 350 l/h. The mass spectrometer was operated in the selected ion monitoring mode using the respective MH⁻ ions, m/z 423.3 for pravastatin and m/z 409.3 for the internal standard. The mobile phase used for high-performance liquid chromatography was acetonitrile/ammonium acetate buffer (10 mM), pH 4 = 7:3 (v/v), and the flow rate was 0.3 ml/min. Chromatographic separation was achieved on a C18 column (Inertsil ODS-3 column, 50×2.1 mm; particle size, 3 μm) (GL Sciences, Tokyo, Japan).

Data Analysis of Metabolic Clearance in Liver S9

The metabolic velocity was calculated from the slope of the natural log (concentration)-time plot. Because the Eadie-Hofstee plot showed curvature, the kinetic parameters were obtained using eq. 1:

$$v = \frac{V_{\max 1} \times S}{K_{m1} + S} + \frac{V_{\max 2} \times S}{K_{m2} + S} \quad (1)$$

where v is the initial velocity (picomoles per minute per milligram of protein), S is the substrate concentration (micromolar), $V_{\max 1}$ and $V_{\max 2}$ are the maximum velocities (picomoles per minute per milligram of protein), and K_{m1} and K_{m2} are the Michaelis constants (micromolar). Fitting was performed with the nonlinear least-squares method using the MULTI program (Yamaoka et al., 1981).

The input data were weighted as the reciprocals of the observed values, and the Damping Gauss-Newton algorithm was used for fitting.

Model Development

The PBPK model was constructed to describe the pharmacokinetics of pravastatin in rats and humans (Fig. 1). The key features of this model are as follows. 1) Active uptake (PS_{int}) and passive diffusion clearances (PS_{diff}) on the sinusoidal membrane, and biliary clearance (PS_{bile}) on the canalicular membrane in the liver are incorporated. 2) The liver compartment consists of five units of extracellular and subcellular compartments, connected by blood flow in tandem, to fit the hepatic disposition to the "dispersion" model. Because the hepatic elimination of pravastatin in rats is blood flow limited, the dispersion model is the appropriate model for the hepatic elimination of such high-clearance drugs (Roberts and Rowland, 1986; Iwatsubo et al., 1997; Naritomi et al., 2001). The number of liver compartments was determined by comparing the hepatic availability ($F_{h,n}$) and F_h predicted using the dispersion model. $F_{h,n}$ is the product of the availability in the liver compartments (eq. 2).

$$F_{h,n} = (Q/(Q + f_B(\text{CL}_{\text{int,all}}/n)))^n \quad (2)$$

where n represents the number of compartments. The integer number n , which gave the $F_{h,n}$ value closest to that in the dispersion model, was selected. 3) The brain and muscle, target tissues for the adverse effects of statins, were included. 4) Although urinary excretion is a minor elimination pathway in male rats, the kidney was included because the kidney/blood concentration ratio for pravastatin is high in male rats, probably because of the efficient uptake and/or reabsorption of pravastatin. The renal clearance of pravastatin in male rats was lower than the glomerular filtration rate corrected by the blood unbound fraction. In contrast, renal clearance must be taken into consideration in humans. Because this study focused on hepatobiliary transport, renal elimination occurs from the systemic compartment. 5) The rapid equilibrium distribution of pravastatin between the blood and tissues other than the liver was assumed. 6) The initial distribution volume, estimated by fitting the plasma concentration time profiles of pravastatin in rats after the

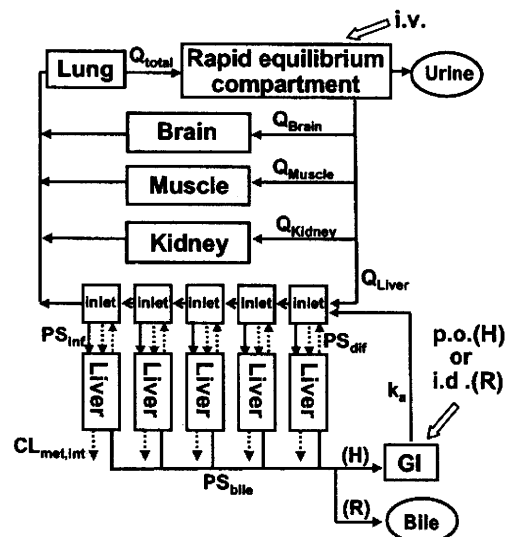


Fig. 1. Schematic diagram of the PBPK model predicting the concentration-time profiles of pravastatin. The liver compartment was divided into five compartments to mimic the dispersion model. Indicated are the blood flow (Q), the active hepatic uptake clearance (PS_{int}), the passive diffusion clearance (PS_{diff}), the biliary clearance (PS_{bile}), and the metabolic clearance ($\text{CL}_{\text{met,int}}$), human (H), and rat (R). The enterohepatic circulation was incorporated in the case of humans.

intravenous administration of 0.2 and 1 mg/kg to a two-compartment model, was used as the volume of the rapid equilibrium compartment including the blood compartment, and it was assumed that there is no interspecies difference in the initial distribution volume. The differential equations are shown in Appendix I, and all simulations were performed with SAAM II (SAAM Institute, Seattle, WA).

Estimation of Kinetic Parameters Used in the Simulation

In Vitro Parameters (Rats and Humans). The in vitro active uptake ($PS_{inf,vitro}$) and passive diffusion clearances ($PS_{dif,vitro}$) of pravastatin on the sinusoidal membrane were determined from the uptake studies using isolated hepatocytes. The parameters for rats were taken from previous reports (Yamazaki et al., 1993; Ishigami et al., 1995), and those for humans were determined in the present study. $PS_{inf,vitro}$ and $PS_{dif,vitro}$ were regarded as the saturable and nonsaturable components, respectively, in the uptake clearance into hepatocytes. A physiological scaling factor of 1.2×10^6 cells/g liver was used for scaling up to the organ level (Iwatsubo et al., 1997). The in vitro biliary clearance ($PS_{bile,vitro}$) of pravastatin was calculated from the ATP-dependent uptake clearance into the CMVs using eq. 3 (Niinuma et al., 1999):

$$PS_{bile,vitro} = (V_{initial} \times R)/(E \times IO) \tag{3}$$

where $V_{initial}$ represents the velocity of the initial ATP-dependent uptake by CMVs corrected by medium concentration (6.08 μ l/min/mg protein for rats and 1.90 μ l/min/mg protein for humans), R represents the recovery of liver homogenate protein (174 mg homogenate protein/g liver for rats and 133 mg homogenate protein/g liver for humans), E represents the enrichment of the CMV fraction (70.4 for rats and 61.8 for humans), and IO represents the population of inside-out CMVs (0.347 for rats and 0.555 for humans).

In Vivo Parameters (Rats). The in vivo intrinsic biliary clearance ($PS_{bile,vivo}$) at the canalicular membrane was calculated by dividing the biliary excretion rate by the hepatic unbound concentration at steady state (Yamazaki et al., 1996b, 1997). Systemic elimination other than biliary excretion was regarded as the hepatic metabolism because renal elimination in male rats is negligible. Thus, in vivo intrinsic metabolic clearance ($CL_{met,int,vivo}$) was obtained with eq. 4:

$$CL_{met,int,vivo} = PS_{bile,vivo}$$

$$\times \frac{100 - (\% \text{ of excretion into bile at } 0.2\text{mg/kg})}{(\% \text{ of excretion into bile at } 0.2\text{mg/kg})} \tag{4}$$

The in vivo passive diffusion clearance on the sinusoidal membrane was assumed to be the same as $PS_{dif,vitro}$. The in vivo active uptake clearance ($PS_{inf,vivo}$) was estimated using eq. 5:

$$PS_{inf,vivo} = CL_{int,all} \times \frac{PS_{dif,vivo} + PS_{bile,vivo} + CL_{met,int,vivo}}{PS_{bile,vivo} + CL_{met,int,vivo}} - PS_{dif,vivo} \tag{5}$$

where $CL_{int,all}$ represents the overall hepatic intrinsic clearance estimated from the hepatic availability using the dispersion model, with a dispersion number of 0.17, which was obtained by dividing the bioavailability by the fraction absorbed (Komai et al., 1992), assuming negligible metabolism in the small intestine. The average of the tissue/blood concentration ratios at 30, 60, and 90 min after the intravenous administration at 10 mg/kg pravastatin were used as the tissue/blood partition coefficient (K_p), assuming a pseudo-steady state (Table 2). Actually, the tissue/blood concentration ratios at 30, 60, and 90 min were similar (muscle, 0.28, 0.21, and 0.18; brain, 0.045, 0.029 and 0.034; kidney, 13, 14, and 15; lung, 0.76, 0.67, and 0.77 at 30, 60, and 90 min, respectively). The absorption rate constants were estimated by noncompartment analysis using the plasma concentration data.

Results

In Vivo Pharmacokinetics of Pravastatin in Rats.

Figure 2 shows time profiles of the plasma concentration of pravastatin after its intravenous (0.2 mg/kg) and intraduodenal (20 mg/kg) administration and the cumulative amount of pravastatin excreted into the bile. The total blood clearance ($CL_{tot,B}$) was similar to the hepatic blood flow rate. The bioavailability of pravastatin after intraduodenal administration was calculated to be 0.0087 by comparing the AUC for pravastatin after intravenous and intraduodenal administration. Forty-six percent of the dose was recovered in the bile as the parent compound after intravenous administration, whereas the amount excreted into the urine was less than 4% of the dose. Even after intraduodenal administration, 33% was recovered in the bile.

The nonlinearity of the disposition of pravastatin was examined. The plasma concentrations and cumulative amounts excreted into the bile after its intravenous administration were determined at doses ranging from 0.2 to 200 mg/kg (Fig. 3). $CL_{tot,B}$ was independent of the dose up to 50 mg/kg but decreased to 27 ml/min/kg at 200 mg/kg pravastatin. The cumulative biliary excretion increased slightly from 46 to 60% at doses above 0.2 mg/kg and was significantly delayed at 200 mg/kg.

Hepatic Metabolism of Pravastatin in Rats. The metabolism of pravastatin in the liver was examined using S9 fractions prepared from rat liver. It exhibited biphasic kinetics with high-affinity (K_m1 , $0.846 \pm 0.403 \mu$ M; V_{max1} , 4.47 ± 1.92 pmol/mg/min) and low-affinity (K_m2 , $80.3 \pm 12.6 \mu$ M; V_{max2} , 240 ± 16.2 pmol/mg/min) components (mean \pm S.D.). The sum of the in vitro metabolic clearance for the high- and low-affinity components, corrected with the physiological scaling factor of 96.1 mg protein/g liver, was used as the in

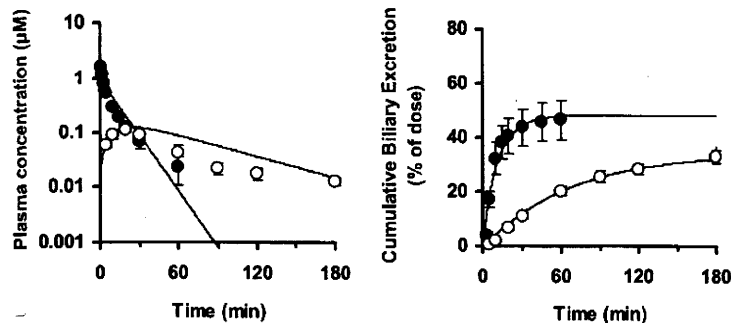


Fig. 2. Simulated and observed plasma concentrations and biliary excretion rates for pravastatin in rats after intravenous (●, 0.2 mg/kg) or intraduodenal (○, 20 mg/kg) administration. The symbols and solid lines represent experimentally observed and simulated values, respectively. Each point represents the mean \pm S.E. ($n = 3$).

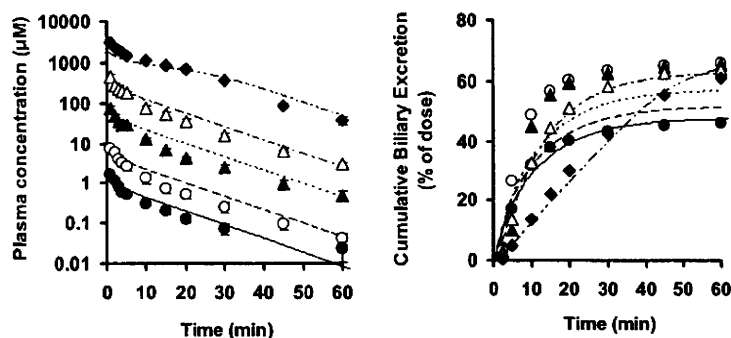


Fig. 3. Simulated and observed plasma concentrations and biliary excretion rates for pravastatin in rats after the intravenous administration of various doses. The symbols and lines represent experimentally observed and simulated values, respectively. Each point represents the mean \pm S.E. ($n = 3$). —●—, 0.2 mg/kg; —○—, 1 mg/kg; —□—, 10 mg/kg; —△—, 50 mg/kg; —◇—, 200 mg/kg.

vitro metabolic clearance ($CL_{met,int,vitro}$), which was 0.793 ml/min/g liver (Table 1).

Simulation of Concentration-Time Profiles of Pravastatin in Rats. All parameters used in the simulation are summarized in Tables 1 and 2. The initial distribution volume was estimated to be 0.393 l/kg from the plasma concentration profile after the intravenous administration of 0.2 mg/kg pravastatin, which was used as the volume of the rapid equilibrium compartment in the model. Figures 2 and 3 show the simulated plasma concentrations and biliary excretion time profiles for pravastatin, together with the observed data after its intravenous and intraduodenal administration. To reproduce the in vivo pharmacokinetic profiles using in vitro parameters, SFs were necessary. For the in vitro-in vivo extrapolation of the transporter-mediated clearances, the ratio of the in vivo/in vitro intrinsic clearances of each process in rats was given as the SF (Table 1). Furthermore, using the K_m values, the simulated plasma concentration and biliary excretion time profiles gave similar values to the observed data, even under nonlinear conditions. This model reproduced the time profiles for pravastatin in the liver and other peripheral tissues after its intravenous administration (Figs. 4 and 5). In particular, the nonlinearity of the liver concentration-time profiles could also be simulated (Fig. 4). Although the model reasonably describes the experimental data, the simulated lines showed some deviation from the observed data at the terminal phase in Figs. 2 (left)

and 5. This may be caused by the lack of a compartment corresponding to the organ, which is associated with the terminal phase of systemic pravastatin. Moreover, the simulation results of biliary excretion of pravastatin administered at 1 and 10 mg/kg showed some deviation from the observed data (Fig. 3, right). Because hepatic metabolism is saturated at these doses, this may be attributed to the deviation of the K_m value for metabolism.

Prediction of Pharmacokinetics in Humans. The uptake clearance determined using eight lots of human cryopreserved hepatocytes was $4.5 \pm 2.9 \mu\text{l}/\text{min}/10^6$ cells at $1 \mu\text{M}$ pravastatin and $0.77 \pm 0.63 \mu\text{l}/\text{min}/10^6$ cells at $100 \mu\text{M}$ pravastatin (mean \pm S.D.). Using the physiological scaling factor of 1.2×10^9 cells/g liver, $PS_{inf,vitro,human}$ and $PS_{dif,vitro,human}$ were calculated to be 0.448 and 0.0924 ml/min/g liver, respectively (Table 1). Unlike the rat liver S9 fraction, no metabolism of pravastatin was observed up to 180 min in the human liver S9 fractions purchased from three different vendors. Thus, the hepatic metabolism of pravastatin might be negligible in the human liver. The in vivo kinetic parameters for pravastatin in humans were predicted by multiplying the corresponding in vitro parameters obtained using human materials by the SF obtained from rat studies. For PS_{bile} , the saturable (ATP-dependent) biliary clearance in humans was predicted as described above (eq. 3), and the nonsaturable component of the biliary clearance in humans was assumed to be the same as that in rats. Thus, the predicted $PS_{bile,vivo,human}$ was 0.388 ml/min/g

TABLE 1

Kinetic parameters for hepatic intrinsic clearance

Active hepatic uptake and passive diffusion clearances on the sinusoidal membrane, biliary clearance on the canalicular membrane, and metabolic clearance were estimated by both in vitro and in vivo experiments. The details of these estimations are described in the text. Values within parentheses indicate the K_m value (micromolar) for each clearance.

	Rat		Scaling Factor	Human	
	In Vitro	In Vivo		In Vitro	In Vivo*
	<i>ml/min/g liver</i>				
PS_{inf}	2.47 ^{a,b} (32.8)	9.06 ^c	3.7	0.448	1.66
PS_{dif}	0.192 ^{a,b}	0.192 ^c	1 ^c	0.0924	0.0924
PS_{bile}					
ATP-dependent	0.0433 ^c	0.906 ^d (92.3)	21	0.00737 ^c	0.154
Nonsaturable		0.234 ^e			0.234 ^f
$CL_{met,int}$	0.793 (0.846, 80.3)	1.33 ^g	1.7	0	0

* Predicted by multiplying the in vitro parameter by the SF.

^a Yamazaki et al. (1993).

^b Ishigami et al. (1995).

^c Calculated using eq. 3 (Niinuma et al. (1999)).

^d Yamazaki et al. (1997).

^e Assumed that the SF for PS_{dif} is 1.

^f Assumed negligible interspecies difference between rat and human.

^g Calculated using eq. 5.

^h Calculated using eq. 4.

TABLE 2
Physiological and kinetic parameters for modeling in rats and humans

	Rat	Human
Physiological Parameters		
Weight (g/kg) ^a		
Liver	41.2	24.1
Extracellular space in liver	11.5	6.7
Brain	6.8	5.3
Lung	4.0	16.7
Muscle	488	429
Kidney	9.2	4.43
Blood flow rate ^a (ml/min/kg)		
Liver	55.2	20.7
Brain	5.3	10.0
Lung	172	74.9
Muscle	30.0	10.7
Kidney	36.9	15.7
Kinetic parameters		
Plasma unbound fraction ^b	0.64	0.47
Liver unbound fraction	0.51 ^c	0.51 ^d
Blood/plasma ratio ^e	0.59	0.56
Fraction absorbed	0.62 ^f	0.47 ^g
Renal clearance (ml/min/kg)	1.5 ^h	11.3 ⁱ
Absorption rate constant (min ⁻¹) ^j	0.0088	0.0078
Tissue/blood concentration ratio		
Brain	0.036	0.033 ^k
Lung	0.74	0.67 ^k
Muscle	0.22	0.20 ^k
Kidney	14	13 ^k

^a The volume and blood flow rate in each tissue were taken from Davies and Morris (1993) and Kawai et al. (1994). The tissue volume was converted to tissue weight based on the assumption that the tissue gravity is 1 g/ml.

^b Yamazaki et al. (1996c) and manufacturer's interview form.

^c Yamazaki et al. (1996b).

^d Assumed negligible interspecies difference between rat and human.

^e Yamazaki et al. (1996c) and Lennernäs and Fager (1997).

^f Komai et al. (1992).

^g Estimated from the bioavailability (0.18) and hepatic availability (0.38) (Singhvi et al., 1990).

^h Obtained from the urinary excretion data for intravenous administration of 10 mg/kg.

ⁱ Singhvi et al. (1990).

^j Estimated by noncompartment analysis.

^k Estimated by $K_p = f_B/f_T$.

liver. Assuming that the distribution of pravastatin to the tissues, except the liver, occurs by passive diffusion, the tissue/blood partition coefficient (K_p) was calculated by the following equation: $K_p = f_B/f_T$, where f_B and f_T represent the blood unbound fraction (=plasma unbound fraction/blood-to-plasma concentration ratio) and the unbound fraction in the tissues, respectively. It was assumed that there is no species difference in f_T between rats and humans based on the previous report by Sawada et al. (1985). The estimated or reported physiological, anatomical, and kinetic parameters for humans used in the simulation are shown in Tables 1 and 2. Using these parameters, the plasma concentration-time profiles for pravastatin in humans after intravenous or oral administration were predicted. A lag time of 17 min was taken into consideration in the simulation of oral administration. The predicted concentration-time profiles were similar to the observed data (Fig. 6).

Effect of Transporter Activity on Systemic and Target Exposure. Sensitivity analyses were performed to understand the effects of the changes in transporter activities on the time profiles for the plasma and liver (a target organ) concentrations of pravastatin in humans. The plasma and liver concentrations after the oral administration (40 mg) of pravastatin were simulated using the PBPK model constructed in this study, with varying hepatic transport activities over a range of 0.33 to 3.0 times the initial value. The simulated concentration-time profiles and the changes in the

AUC are shown in Fig. 7 and Table 3, respectively. Changes in the active hepatic uptake ability affected the plasma concentration profiles dramatically but did not greatly affect the liver concentration profiles. On the contrary, changes in the ability of canalicular efflux altered the liver concentration of pravastatin markedly but had a small effect on the plasma concentration. Changes in the passive diffusion clearance hardly affect the plasma and the liver concentration profiles.

Discussion

It is now well recognized that drug transporters play important roles in the processes of absorption, distribution, and excretion (Giacomini and Sugiyama, 2005; Shitara et al., 2006a). The purpose of this study was to construct a PBPK model to evaluate the concentration-time profiles for drugs in the plasma and peripheral organs in humans using physiological parameters, SFs, and drug-related parameters (unbound fraction and metabolic and membrane transport clearances extrapolated from in vitro experiments). The principle of the prediction was as follows. First, SFs were obtained by comparing in vitro and in vivo parameters in rats. Then, the in vitro human parameters were extrapolated in vivo using the SFs obtained in rats (Naritomi et al., 2001). Pravastatin was selected as the model compound because many studies have investigated the mechanisms involved in the drug disposition in rodents, and clinical data after intravenous and oral administration are available.

Consistent with a previous report (Yamazaki et al., 1996a), the hepatic elimination of pravastatin is blood flow limited. Considering that the maximum amount of intact pravastatin excreted into the bile was 50%, it is likely that pravastatin undergoes hepatic metabolism in rats because pravastatin is excreted negligibly in the urine. Incubating pravastatin with the rat liver S9 fractions caused a reduction in intact pravastatin with time and consisted of two different mechanisms with high- and low-affinity sites. The kinetic parameters related to hepatic clearance (PS_{inb} , PS_{dif} , PS_{bile} , and $CL_{met,int}$) were estimated from various in vivo experiments and were incorporated into the PBPK model. As a result, plasma concentration and biliary excretion-time profiles for pravastatin were successfully reproduced (Figs. 2–5). Moreover, nonlinear pharmacokinetics were also reproduced using the K_m values for hepatic uptake, biliary excretion, and metabolic clearances (Fig. 3). The liver concentrations of pravastatin were similar to the observed data,

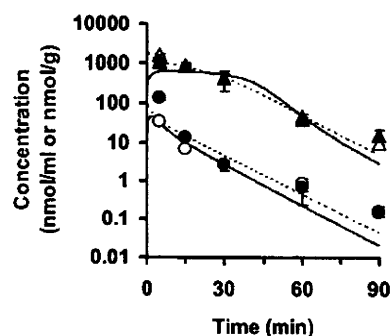


Fig. 4. Simulated and observed liver concentration profiles for pravastatin in rats after intravenous administration. Dashed and solid lines, simulated plasma and liver concentrations, respectively. Open and closed symbols, experimentally observed plasma and liver concentrations, respectively (circles, 10 mg/kg; triangles, 200 mg/kg). Each point represents the mean \pm S.E. ($n = 3$).